JOC The Journal of Organic Chemistry

Article

pubs.acs.org/joc

Synthesis and Photophysical Properties of Aza[*n*]helicenes

Gourav M. Upadhyay, Harish R. Talele, and Ashutosh V. Bedekar*

Department of Chemistry, Faculty of Science, M. S. University of Baroda, Vadodara 390 002, India

Supporting Information

ABSTRACT: Synthesis and study of aza[7]helicene and aza[9]helicene is presented in this paper. Photo-dehydrocyclization of the 3,6-bis-styryl derivative of carbazole leading to sterically less demanding aza[7]helicene resulted in smooth reaction, and only the desired angular−angular product was detected. However, in the case of aza[9]helicene, along with the expected angular−angular cyclization, three other products involving linear mode of cyclization were also isolated and characterized. In this case, the helical compound aza[9]helicene was predominantly formed at lower concentration while the other isomers were obtained at higher concentration. All of the compounds formed by angular−angular, angular−linear, and linear−linear modes of cyclization were fully characterized, and their photophysical properties were investigated.

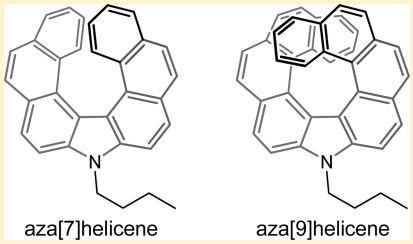

INTRODUCTION

Helicenes, due to their fascinating structures and associated distinct properties, have been the subject of considerable research in recent years. These molecules acquire a unique screw shape in order to release the internal strain created due to increasing number of rings. There exists a possibility of continuous delocalization of electrons due to aromatic rings fused together in a particular way. The helical molecules can show some unique chiroptical properties due to their special structural arrangements and therefore has been a focus of intense research in recent decades.[1] There are two types of helical molecules: carbohelicenes and heterohelicenes. Initial research was concentrated on carbohelicenes, but recently more interesting properties have been observed for the heterohelicenes containing one or more different heteroatoms.

Helicenes with the possibility of continuous delocalization of electrons and tunable planarity are potential substrates for study of their photophysical properties. The different types of helical systems have been investigated with exciting photophysical properties such as luminescence,[2] circularly polarized luminescence,[3] fluorescence,[4] circular dichroism,[1a,5] etc. Some of the optical properties of helicenes are well documented in excellent reviews.[1h,6]

The presence of a heteroatom in the fused polycyclic systems considerably contributes to altering the electronic structure and helps fine-tune various optoelectrical properties. For example, thiahelicenes containing benzene and thiophene rings are expected to have more effective conjugation and electron-donating properties compared to carbohelicenes. A large number of such compounds have been synthesized and studied extensively. For example, esathia[11]helicene **I** has been synthesized, and its electronic and self-assembling properties have been investigated[7] (Chart 1). Polycyclic aromatic oxygen containing molecules, particularly fused furans, are expected to provide relatively high HOMO levels[8] and are known to show interesting utility in electronic devices, such as organic light-emitting diodes (OLEDs)[9a] or organic field-effect transistors (OFETs).[9b,c] Recently, we have reported the synthesis of a large 7,12,17-trioxa[11]helicene **II** and studied its photophysical and thermal properties.[10] The presence of silicon improves the luminescence and electron-transport properties of the molecules. It is clearly evident in the synthesis and study of sila[7]helicene **III**, where the changes are linked to changes in physical properties.[2a] Analogous to this is λ^5-phopha[7]helicene **IV**, which is obtained in chirally pure form and shows very high optical rotation, good photoluminescence, and interesting crystal-packing arrangement.[11] Heterohelicenes with nitrogen as heteroatom, referred to as azahelicenes, can be of several types: pyridine-containing, pyridazine, pyrrole derivatives, etc. The pyrrole type is similar to the above molecules and has attracted some interest in recent years[12] along with similar bis-azahelicene.[13] A derivative of the former type aza[7]helicene **V**

Chart 1. Structurally Similar Heterohelicenes

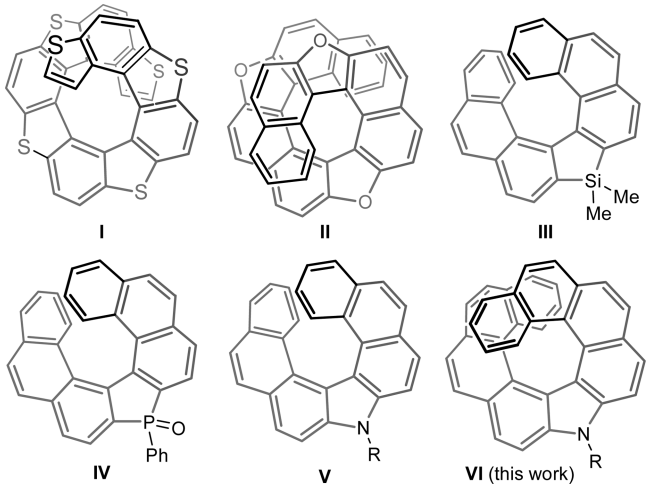

Received: June 14, 2016
Published: July 21, 2016

DOI: 10.1021/acs.joc.6b01395
J. Org. Chem. 2016, 81, 7751−7759

has been synthesized and studied for its photophysical properties, and it also shows remarkably high thermal stability.[12d] The optical properties can be attributed to the extended conjugation created by the *ortho*-fused aromatic rings; hence its analogue aza[9]helicene **VI** is expected to further enhance the conjugation and the photophysical response and may also affect the thermal properties. However, the construction of such a large helicene consisting of nine rings making almost one and half turn of the helix is a challenging task, and its synthesis is not reported in the literature. In this paper, we discuss the synthesis of aza[7]helicene and aza[9]helicene and present preliminary studies of the photophysical properties. Although structurally similar, the two helical compounds substantially differ in the internal strain caused by the steric crowding and offer different degrees of challenge in their synthesis.

RESULTS AND DISCUSSION

We have adopted the method of photodehydrocyclization of appropriate bis-stillbene derivatives of carbazole to accomplish the formation of aza[*n*]helicene (*n* = 7 or 9). The smaller derivative aza[7]helicene should offer less internal steric crowding and should result in facile cyclization; however, the larger aza[9]helicene should offer considerably more internal strain and may pose difficulty in the desired cyclization. A detailed investigation on the mode of photocyclization of stillbene derivatives leading to carbohelicenes has been reported previously[14] where a comparison between the angular and linear path has been elaborated. In cases where the photocyclization can occur at two different sites of a polynuclear system, the regiochemistry is controlled by two major considerations, the electronic and steric factors.[15] If steric hindrance is not very severe then the product is usually formed through the intermediate, which will lead to greater aromatic resonance stabilization. When the electronically favorable pathway is considerably sterically hindered, then the less hindered alternative pathway is preferred.[16a] In some cases, the regioselectivity in such photocyclizations can be predicted by molecular orbital calculations of the difference in excited-state free-valence indices and Mulliken electronic overlap populations at the two sets of carbon atoms involved in ring closure. However, in some cases, even though the favorable theoretical predictions are made, the actual photocyclization may result in failure.[17] In the analogous case of photocyclization of carbazole-based stillbene derivatives, the two available sites may direct the photocyclization leading to either angular or linear isomer. This type of the two modes of cyclization of **VII** has also been discussed in a previous study,[18] explaining the formation of the two isomers resulting at electrocyclization at the a or b position (Scheme 1). The position a is electronically more favorable for electrocyclization compared to position b. The two possible dihydro intermediates **VIIIa** and **VIIIb** would on oxidation give aromatized angular product **IXa** and linear product **IXb**. In the angular case, the intermediate **VIIIa** retains the aromatic character of the pyrrole ring of the carbazole moiety, while it is compromised in the intermediate **VIIIb** in linear mode. This case is analogous to the intermediates proposed by Katz et al.[18] for the Diels–Alder cycloaddition of vinyl carbazole, where the intermediate for the angular reaction was calculated to be 8.6 kcal/mol more stable than the corresponding linear intermediate.

The first type of angular cyclization on two sides of carbazole should lead to aza[*n*]helicene, the target molecule of the present study. Our initial efforts have been focused on the synthesis of aza[7]helicene and its derivatives.[12d] To increase the solubility of the resultant aza[7]helicene the *n*-Bu group was selected.[19] The synthesis of **4** was achieved by a combination of a Heck reaction followed by a standard photocyclization procedure (Scheme 2).[20] Careful analysis of the reaction mixture revealed consumption of the starting material and formation of a major product, which was isolated by column chromatography over silica gel. The ^{1}H NMR analysis of the crude reaction mixture clearly established the

Scheme 1. Two Possible Modes of Photocyclization

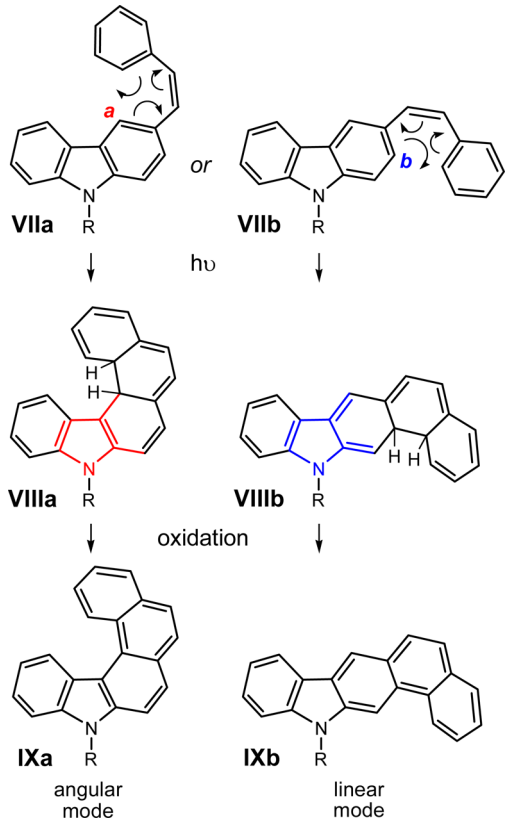

Scheme 2. Synthesis of Aza[7]helicene 4

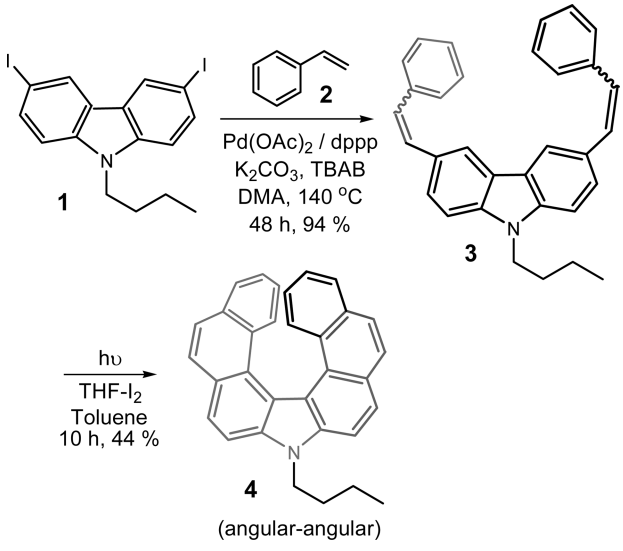

DOI: 10.1021/acs.joc.6b01395
J. Org. Chem. 2016, 81, 7751–7759

Scheme 3. Photodehydrocyclization of Bis-stilbenoid Derivative 6

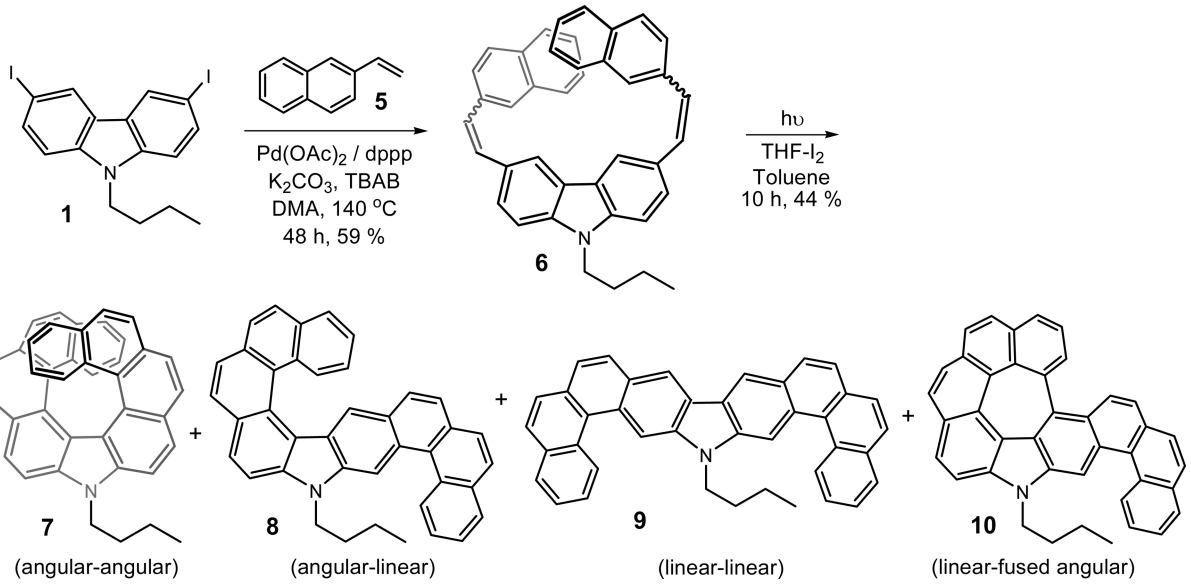

double-angular cyclization **4** as the sole product (see the Supporting Information). This observation differs slightly from the earlier Diels–Alder case[18] where the authors reported two products of aza[7]helicene formed through angular–angular and angular–linear reactions, while the product due to a linear–linear reaction path was completely absent.

The synthesis of the desired aza[9]helicene should be similarly achieved by simultaneous double photo-dehydrocyclization of 3,6-bis(2-(naphthalen-2-yl)vinyl)carbazole **6**, analogous to the synthesis of aza[7]helicene.[12d] Accordingly, the 3,6-diiodo-*N*-butylcarbazole **1** was converted to bis-olefin **6** by its Mizoroki–Heck reaction[21] with vinylnaphthalene **5**. A solution of **6** in toluene was subjected to photochemical reaction (125 W HPMV lamp) in a standard immersion well reactor (Scheme 3).[20]

The initial analysis of the reaction mixture indicated the formation of a complex mixture of the products, contrary to the earlier observation of aza[7]helicene. This is probably due to the different possible modes of cyclization of the intermediate species in the stilbenoid derivative (Scheme 4). In this reaction, two conflicting forces control the regiochemistry of cyclization, the electronic considerations and steric factors. The electronic effects of retaining the aromatic character of the pyrrole ring in **Xa** direct the cyclization in an angular manner. However, this effect is partially balanced by the steric effect created by an additional aromatic ring of naphthalene unit favoring the formation of intermediate **Xb**, leading to the linear mode of cyclization. Based on this hypothesis, we anticipate the formation product resulting in a linear mode of cyclization. The cyclization in the present bis-stilbenoid derivative **6** may follow in a stepwise manner; the regiochemistry of the second cyclization will be controlled by the first reaction. If the initial cyclization follows the angular path, an intermediate **XIa** will be formed that may give two possible regioisomers (angular–angular **7** and angular–linear **8**) during the second reaction. On the other hand, if the initial cyclization gives linear isomer **XIb**, the second cyclization can result in the formation **8** or **9**.

Careful purification of the reaction mixture furnished four distinct products, which were adequately characterized by spectroscopic and analytical techniques (Figure 1). The

Scheme 4. Possible Intermediates in the Photodehydrocyclization of 2-((Naphthalen-2-yl)vinyl)carbazole

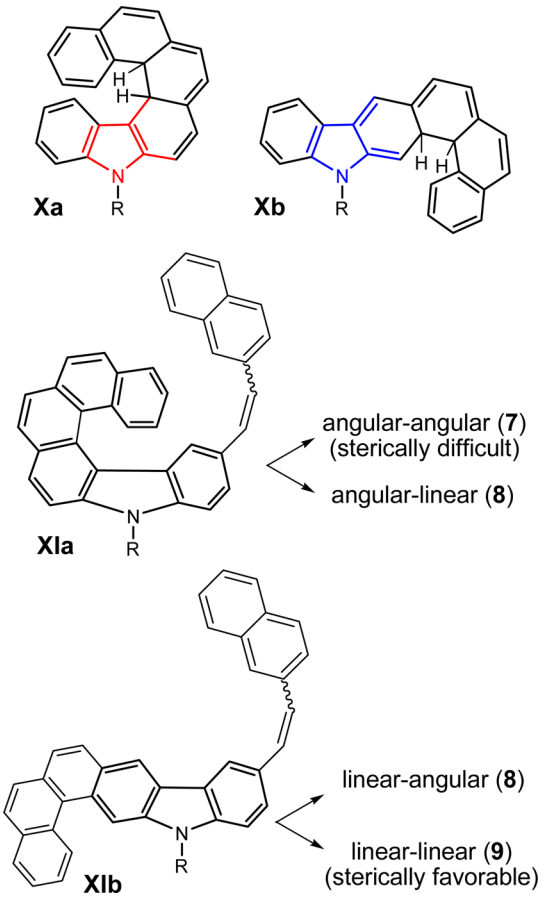

structures **7**–**10** were assigned by ^{1}H NMR spectra. The compound **7** showed a symmetrical pattern without any singlet. The hydrogen attached to C1 appeared in the upfield aromatic region because it was in the ring current of the last aromatic ring and showed as a doublet at δ 6.11 ppm, while the hydrogen

DOI: 10.1021/acs.joc.6b01395
J. Org. Chem. 2016, 81, 7751–7759

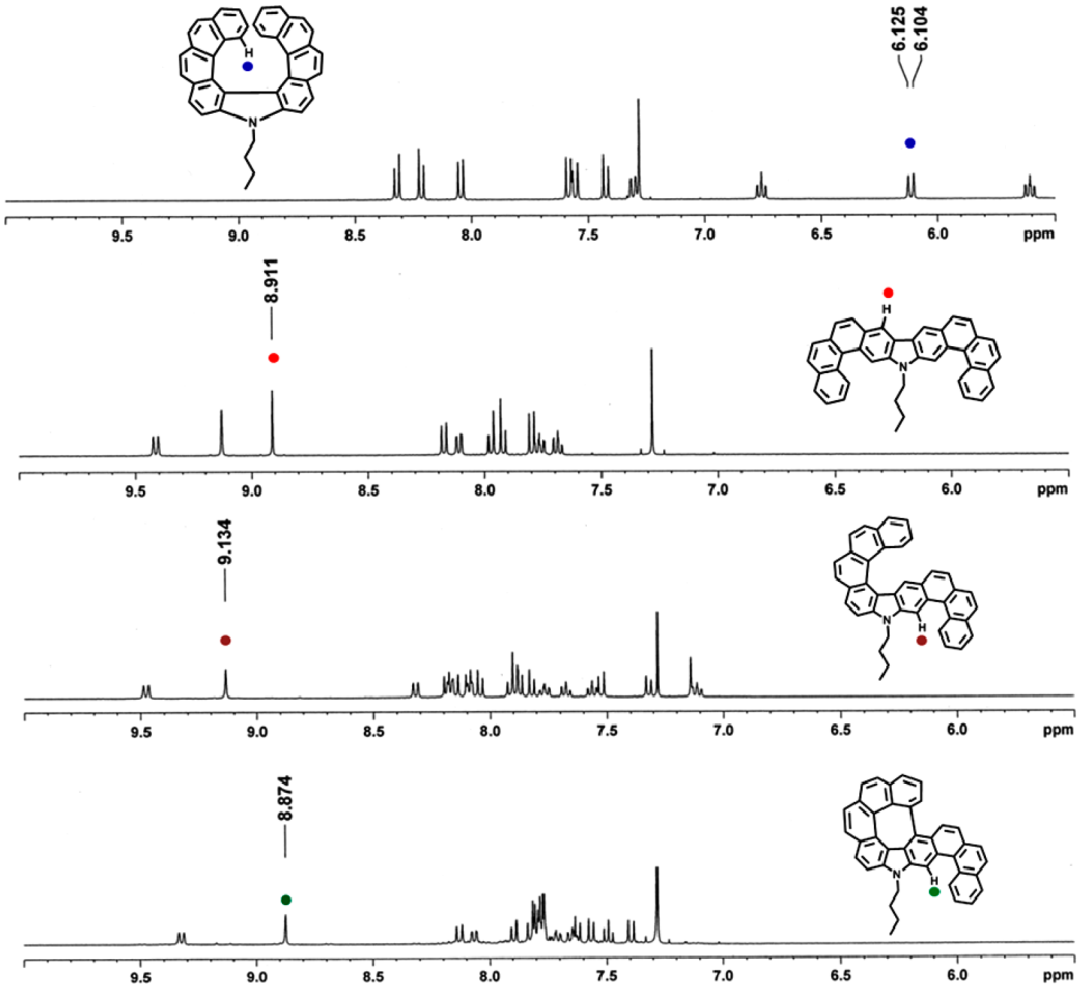

Figure 1. Comparison of the ^{1}H NMR data of four isomers 7−**10** (400 MHz in $CDCl_3$).

attached to C2 appeared most upfield in the aromatic region at δ 5.60 ppm as a multiplet (see the SI for the numbering system). The angular−linear isomer **8** shows an unsymmetrical pattern resulting in more signals. Typically, the hydrogen attached to C1 of the aza[6]helicene part of the molecule appeared in the upfield region at δ 7.32 ppm as a doublet and hydrogen at C2 as a multiplet at δ 7.11 ppm. The linear part of the molecule is established by observing the hydrogen attached to C20 as a doublet at δ 9.47 ppm and the corresponding two singlets for hydrogens attached to C12 and C21 at δ 7.14 and 9.13 ppm, respectively. The linear−linear isomer **9** also showed a symmetrical pattern in the ^{1}H and ^{13}C NMR. The hydrogens attached to C9 and C21 appeared as singlets at δ 8.91 and 9.13 respectively. The hydrogen attached to C1 appeared as doublet at δ 9.41 ppm. The fourth product showed two fewer hydrogens, and we concluded that further oxidation has taken place similar to the formation of benzo[*ghi*]perylene. This compound **10** also showed an unsymmetrical pattern. The absence of hydrogens at C1 and C12 of the aza[6]helicene part of **8** was clearly noted. The only singlet appeared δ 8.87 ppm, corresponding to hydrogen attached to C21. The fourth product **10** appears to be formed where the portion on the angular cyclization part of **8** (aza[6]helicene unit) undergoes further oxidation, resulting in a fused system similar to that of benzo[*ghi*]perylene.[22] It was observed that although the four compounds were detected in the crude sample, their separation proved to be difficult and challenging. Separation of regiomers was done by enrichment of the respective compound using column chromatography followed by fractional crystallization in different solvents. The angular−angular isomer **7** was found to be slightly different in polarity, while the other three were of almost similar nature on TLC (see the Supporting Information for details).

All four compounds were further characterized by single-crystal X-ray diffraction to determine the shape of the molecules arising due to the strain created by building up of the aromatic rings. The crystal structure of **7** indicates a high degree of distortion of the molecular structure, which is a sum of torsion angles ($\varphi1 + \varphi2 + \varphi3 + \varphi4$) equal to 74.22° while the dihedral angle θ was measured to be 41.01° (Figure 2). The two terminal rings were almost parallel to each other; the planes passing through them bisected at an angle of only 7.92°, and the pitch of outer helix was observed to be 3.97 Å. As expected for such helical structures, the outer C−C bonds were slightly reduced in length (1.329 to 1.398 Å) while the inside ones were bit elongated (1.407−1.449 Å) and the inner C−C bond of the pyrrole ring was 1.455 Å.

The other isomer **8** due to angular−linear cyclization has two components; one is the aza[6]helicene fused with the other [4]helicene. Its crystal structure indicates a distortion of the molecular structure on the former side, which is a sum of torsion angles, to be 66.77°, while the dihedral angle θ was measured to be 54.18° (Figure 3). It is generally observed that

DOI: 10.1021/acs.joc.6b01395
J. Org. Chem. 2016, 81, 7751−7759

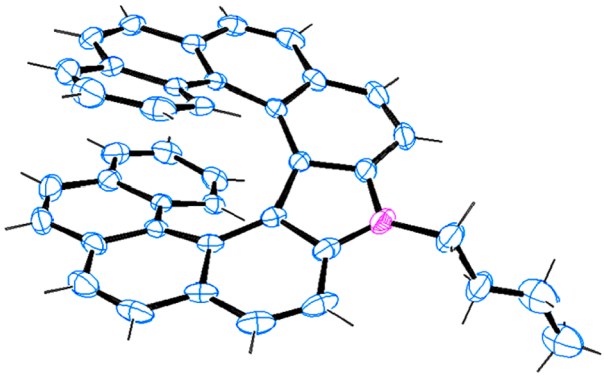

Figure 2. ORTEP diagram of **7**; thermal ellipsoids are drawn at the 30% probability level (CCDC 1025231).

the dihedral angle of smaller helical structures often tend to be larger compared to the more elongated helices.[23]

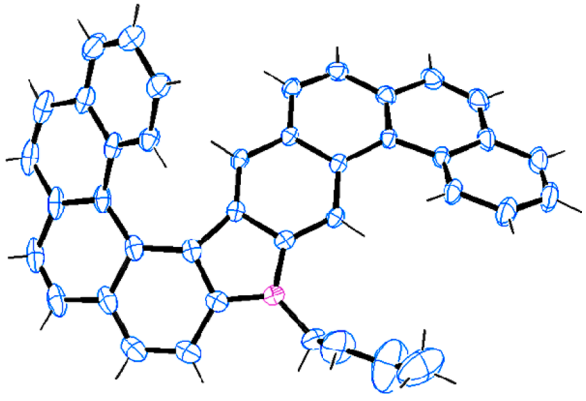

Figure 3. ORTEP diagram of **8**; thermal ellipsoids are drawn at the 30% probability level (CCDC 1439548).

The next isomer isolated in the cyclization is due to the linear−linear mode and also shows an interesting crystal structure (Figure 4). The structure of this molecule closely

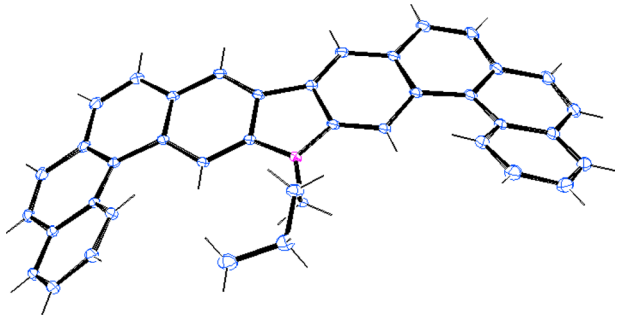

Figure 4. ORTEP diagram of **9**; thermal ellipsoids are drawn at the 30% probability level (CCDC 1025232).

resembles[24c] diphenanthro[4,3-*a*;3′,4′-*o*]picene, which was almost simultaneously synthesized by Martin[24a] and Laarhoven.[24b] Molecule **9** also crystallized in the monoclinic space group of $P2_1/c$ and showed a relatively small torsion angle of about 38° and a dihedral angle of 29.7°.The molecule is like a wing of a bird, and when fully spread measures 16.67 Å in length and about 8.95 Å in width.

The angular−linear product **8** could undergo further oxidation reaction because the two terminal rings of the aza[6]helicene portion were juxtaposed in close proximity. Hence, a much longer extended conjugation is seen in compound **10** compared to the other three molecules. As a result, the dihedral angle of the aza[6]helicene portion reduced to 33.8° as compared to **8** (Figure 5).[25] This molecule appears to acquire a relatively flat shape as compared to the angular−linear derivative.

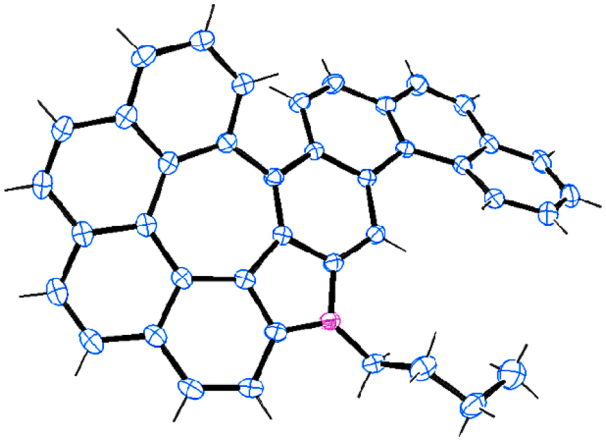

Figure 5. ORTEP diagram of **10**; thermal ellipsoids are drawn at the 30% probability level (CCDC 1036685).

Effect of Concentration on Product Distribution. As mentioned previously, the regiomer formation was dependent mainly on two considerations: steric and electronic factors. Some other factors have been studied to understand the regiomer formation. The composition of regiomers depends on wavelength distribution of the incident light, the reaction temperature,[26] the nature of oxidant, and concentration.[16b] It is believed that the dimer formation is considerably reduced at much higher dilution suppressing the photodimerization process. Hence, it is recommended to carry out photolysis experiments at very high dilution to prevent the dimerization processes (10^{-2} M or less). However, the effect of concentration on the distribution of possible regioisomeric products is rarely investigated.[27]

In the exploratory stage of our current investigation, the ^{1}H NMR analysis of the crude reaction mixture indicated that the distribution of four observed products was concentration dependent, prompting us to investigate this further. As discussed previously, a few signals in the ^{1}H NMR for the four compounds appeared at distinctly different positions, helping us to determine the ratio in crude samples by measuring their quantity[28] (Table 1). It was established from the above study that the desired angular−angular isomer **7** formed predominantly at higher dilution (lower concentration) while the other regiomer formed at higher concentration. The observed ratio can be attributed to the population of excited-state intermediates, their stabilities, and their relative rates for the electrocyclization reactions. This observation of the correlation of concentration and the product distribution may help researchers in planning the synthesis of similar fused systems.

Studies of Photophysical Properties. The absorption and emission spectra of all of the compounds were recorded in dilute solutions of dichloromethane at room temperature

DOI: 10.1021/acs.joc.6b01395
J. Org. Chem. 2016, 81, 7751−7759

Table 1. Effect of Concentration on the Distribution of Products[a]

entry	conc (mol/L)	7 δ = 6.11 (d)	**8** 9.13 (s)	**9** 8.91 (s)	**10** 8.87 (s)
1	150 mg in 1 L(2.86×10^{-4})	60.97	4.87	24.39	9.75
2	250 mg in 1 L (4.78×10^{-4})	38.46	14.61	22.30	24.61
3	500 mg in 1 L (9.56×10^{-4})	18.66	44.77	27.98	8.58
4	800 mg in 1 L (1.52×10^{-3})	14.32	45.27	31.80	8.59
5	1.0 g in 1 L (1.91×10^{-3})	ND	48	52	ND

[a]ND = not detected. Ratios in percent. Ratio determined after normalization, and the overall yield was between 43 and 45%.

(Figure 6). The π conjugation length is almost similar for all four isomers (**7**–**10**), so the shifts in both the absorption and

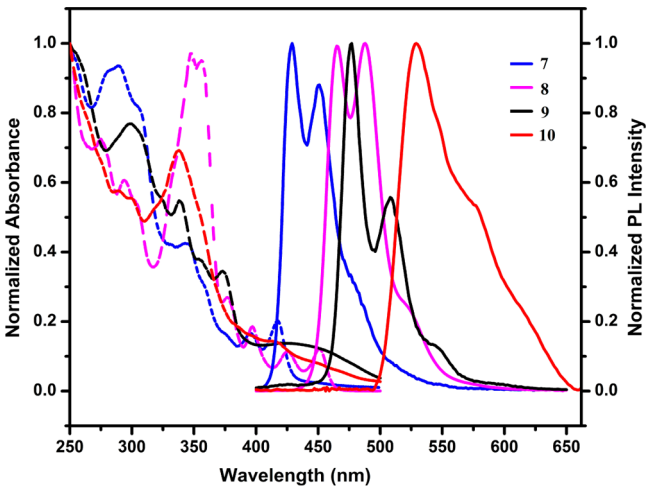

Figure 6. Absorption (dotted line) and emission (solid line) spectra of **7**–**10** in dichloromethane (abs 1×10^{-5} M; em 1×10^{-6} M).

emission spectra can be explained on the basis of effective spread of the π resonance system over the entire molecule. The angular–angular compound **7** exhibited a deep blue emission peak at 429 nm and a shoulder peak at 451 nm. It appeared to show the most blue shift in the emission spectra, reinforcing the highly distorted structure created by helical twist. Such a shape contributes to the non-coplanar geometry, resulting in the reduction of effective π conjugation causing a blue shift in the fluorescence spectra of aza[6]helicene.[2b] Interestingly, the emission maximum for aza[9]helicene was almost similar to the corresponding aza[7]helicene[29] probably due to combination of contradictory effects of distorted geometry (leading to more blue shift) and extended conjugation (resulting in red shift).[2b] The angular–linear compound **8** showed a blue shift compared to the more linear π molecular systems **9** and **10**; this phenomenon might be attributed to the high dihedral angle which limits the delocalization of electrons throughout the molecule to some extent. The compound **9** showed a red shift due to effective delocalization as well as better π–π stacking. The compound **10** showed the maximum bathochromic shift in emission spectra, indicating more effective delocalization of π electrons due to annulation.

The fluorescence quantum yields of four isomers were recorded in dilute dichloromethane solution ($\sim 10^{-6}$ M) at room temperature; data are summarized in Table 2. The Φ (fluorescence quantum yield) of all regiomers were found to be low to moderate (0.07–0.21), which probably indicates that the excitons were not confined to the whole backbone of these molecules due to its nonplanar molecular structure. The reason for moderate quantum yields can be attributed to the marginal

Table 2. Photophysical Properties of 4 and 7–10

compd	λ_{abs} (nm)	λ_{em} (nm) (λ_{exc} (nm))	Stokes shift (nm)	Φ_{FL} (λ_{exc} (nm))
4	262, 329, 337	430, 448 (262)	186	0.17 (366)
7	289	429, 451 (289)	140	0.20 (313)
8	348	465, 488 (348)	117	0.19 (306)
9	299	477, 508 (299)	178	0.21 (363)
10	338	529, 578 (338)	191	0.07 (338)

loss of energy during the exciton migrations.[30a] The quantum yield of the compound **7** was higher than the similar carbo analogue, [9]helicene[30b] (Φ = 0.014) and pentathia[9]-helicene[30c] (Φ = 0.02) and also approximately three times higher than compound **10**, which can be explained by greater steric hindrance in compound **7**. The greater strain and rigidity of **7** also reduces the availability of nonradiative deactivation pathways, forcing the molecule to relax via photon emission.[30d]

Fluorescence quantum yields were determined using a solution of quinine sulfate in H_2SO_4 (0.5 M) as a reference standard (Φ_{FL} = 0.546).

The novelty of the present study is not just the synthesis of larger angularly fused aza[9]helicene and separation and characterization of all the related isomers but to put forward the valuable observation of how concentration may play a significant role in controlling the cyclization. This observation may be useful in planning the synthesis of such systems. The dramatic effect of steric considerations was observed in different modes of cyclization when we compared the preparation of aza[7]helicene and aza[9]helicene.

EXPERIMENTAL SECTION

Chemicals and solvents received from commercial sources were used without further purification. All solvents that were used were stored on oven-dried molecular sieves (4 Å). Thin-layer chromatography was performed on F254 aluminum-coated plates. The spots were visualized under UV light or with iodine vapor. All of the compounds were purified by column chromatography using silica gel (60–120 mesh). Photoreactions were performed in an immersion well photoreactor with a water jacket for cooling with a 125-W high-pressure mercury vapor lamp. All reactions were carried out under an inert atmosphere (nitrogen) unless other conditions are specified. ^{1}H NMR spectra were recorded on a 400 MHz spectrometer (100 MHz for ^{13}C) in $CDCl_3$ as solvent and TMS as internal standard. IR spectra were recorded as KBr pallets, HRMS were recorded with an electrospray ion source and controlled by Xcalibur software, and fluorescence and UV–vis spectra were recorded at room temperature. HPLC was performed using CHIRALCEL OD-H column. For preparation of compounds 3,6-distyryl-9-butyl-9*H*-carbazole (**3**) and *N*-butylaza[7]helicene (**4**) refer to the literature report.[12d]

3,6-Diiodocarbazole. To a round-bottom flask (250 mL, two-neck), equipped with a condenser, was loaded a solution of carbazole (5 g, 29.90 mmol), KI (6.45 g, 38.87 mmol), KIO_3 (6.39 g, 29.90 mmol), acetic acid (100 mL), and deionized water (10 mL). The iodination reaction was continued at 80 °C for 24 h. After being cooled to room temperature, the mixture was filtered and washed with

DOI: 10.1021/acs.joc.6b01395
J. Org. Chem. 2016, 81, 7751–7759

deionized water, saturated sodium carbonate solution, and methanol to afford a white-light gray solid (11.39 g, 91%). The analytical data were in complete agreement with the previously published data.[31a]

9-Butyl-3,6-diiodo-9*H*-carbazole (1). 3,6-Diiodocarbazole (2 g, 4.77 mmol) and powdered potassium hydroxide (1.60 g, 28.65 mmol) were mixed in a flask containing acetone (25 mL). After the mixture was stirred for 30 min, 1-bromobutane (0.98 g, 0.77 mL, 7.16 mmol) was added slowly. The solution was stirred for 5 h at room temperature. After completion of the reaction, the mixture was poured into ice-cold water and extracted with ethyl acetate (3 × 100 mL). The combined organic phase was washed with water and brine and dried over anhydrous sodium sulfate. The solvent was removed under reduced pressure, and the crude product was purified by column chromatography on silica gel using petroleum ether as an eluent to afford a white solid (2.13 g, 94%). The analytical data were in complete agreement with the previously published data.[31a]

2-(Bromomethyl)naphthalene. 2-Methylnaphthalene (2 g, 14.06 mmol) was dissolved in carbon tetrachloride (25 mL) in a round-bottom flask equipped with a magnetic stirrer and reflux condenser. To this solution were added a mixture of *N*-bromosuccinimide (3 g, 16.87 mmol) and benzoyl peroxide (0.17 g, 0.70 mmol). The mixture was stirred in the presence of tungsten filament domestic light for 5−6 h. Completion of the reaction was checked by TLC in petroleum ether. After the reaction was complete, the precipitated succinimide was filtered and the solvent was removed under reduced pressure. Light brown solid (2.2 g, 71%) was obtained after crystallization from a mixture of petroleum ether and ethyl acetate. The analytical data were in complete agreement with the previously published data.[31b]

2-(Naphthalen-2-yl)acetaldehyde. In a 100 mL flask equipped with a reflux condenser were placed 2-(bromomethyl)naphthalene (2 g, 9.05 mmol), hexamethylenetetramine (2.53 g, 18.09 mmol), glacial acetic acid (15 mL), and water (15 mL). This mixture was heated under reflux for 2 h. After the reflux period, concentrated hydrochloric acid (10 mL) was added, and refluxing was continued for an additional 15 min. After cooling, the mixture was extracted with 3 × 100 mL of ethyl acetate. The combined organic phase was washed with water and brine and dried over anhydrous sodium sulfate. The solvent was removed under reduced pressure, and the crude product was purified by column chromatography on silica gel using petroleum ether/ethyl acetate (90:10) as eluent to afford a white solid (1.03 g, 73%). The analytical data were in complete agreement with the previously published data.[31c]

2-Vinylnaphthalene (5). To a stirred solution of methyltriphenylphosphonium iodide (3.90 g, 9.60 mmol) in dimethylacetamide (25 mL) was added potassium carbonate (1.77 g, 12.8 mmol). The mixture was stirred for 15 min, and then 2-(naphthalen-2-yl)acetaldehyde (1 g, 6.40 mmol) was added. The mixture was slowly warmed and heated at 70 °C for 3 h. After completion of the reaction, the mixture was poured into ice-cold water and extracted with 3 × 100 mL of ethyl acetate. The combined organic phase was washed with water and brine and dried over anhydrous sodium sulfate. The solvent was removed under reduced pressure, and the crude product was purified by column chromatography on silica gel using petroleum ether/ethyl acetate (98:02) as eluent to afford a white solid (0.70 g, 71%). The analytical data were in complete agreement with the previously published data.[31d]

9-Butyl-3,6-bis(2-(naphthalen-2-yl)vinyl)-9*H*-carbazole (6). A solution of palladium acetate (0.004 g, 0.021 mmol, 2 mol %) and 1,3-bis(diphenylphosphinopropane) (0.017 g, 0.042 mmol, 4 mol %) was prepared in *N*,*N*-dimethylacetamide (5 mL) under nitrogen atmosphere. The mixture was stirred at room temperature until a homogeneous solution was obtained. This catalyst solution was repeatedly purged by N_2 prior to use.

A two-neck, round-bottom flask was charged with 3,6-diiodo-*N*-butylcarbazole (0.5 g, 1.05 mmol), 2-vinylnaphthalene (0.357 g, 2.31 mmol), dry potassium carbonate (0.581g, 4.21 mmol), TBAB (0.067 g, 0.21 mmol, 20 mol %), and *N*,*N*-dimethylacetamide (10 mL), and the mixture was heated to 100 °C. When the temperature reached 100 °C, the previously prepared Pd catalyst solution was added dropwise, and the mixture was heated to 140 °C for 48 h. After completion of the reaction, the mixture was poured into ice-cold water and extracted with dichloromethane (3 × 100 mL). The combined organic phase was washed with water and brine and dried over anhydrous sodium sulfate. The solvent was removed under reduced pressure, and the crude product was purified by column chromatography on silica gel using petroleum ether/ethyl acetate (90:10−60:40) as eluent to afford a *cis*−*trans* mixture of 9-butyl-3,6-bis(2-(naphthalen-2-yl)vinyl)-9*H*-carbazole. R_f = 0.25 (5:95 EtOAc/petroleum ether). Yield = 0.328 g (59%). Physical state = light yellow amorphous solid. Mp = 204−205 °C. ^{1}H NMR (400 MHz, $CDCl_3$): δ 8.35 (s, 2H), 7.92−7.74 (m, 11H), 7.53−7.34 (m, 10H), 4.34 (t, J = 6.8 Hz, 2H), 1.93−1.89 (m, 2H), 1.47−1.42 (m, 2H), 0.99 (t, J = 7.2 Hz, 3H). $^{13}C\{^1H\}$ (100 MHz, $CDCl_3$): 140.7, 135.4, 133.8, 132.8. 129.9, 128.8, 128.2, 127.9, 127.7, 126.2, 126.0, 125.6, 124.7, 123.5, 123.3, 118.7, 109.1, 43.1, 31.2, 20.5, 13.9. IR (KBr): 3045, 2954, 2859, 1617, 1592, 1481, 1428, 135, 1244, 1148, 957, 888, 861, 811, 643, 584 cm^{-1}. HRMS (TOF MS ES+): m/z calcd for $C_{40}H_{33}N$ $[M + H]^+$ 528.2684, found 528.2685

Photocyclization of 6. In an immersion wall photoreactor (borosilicate glass) equipped with a water cooling jacket and a stir bar, a *cis*/*trans* mixture of 9-butyl-3,6-bis(2-(naphthalen-2-yl)vinyl)-9*H*-carbazole **6** (0.175 g, 0.33 mmol), iodine (0.185 g, 0.73 mmol), and THF (2.39 g, 2.69 mL, 33.2 mmol) was dissolved in toluene (350 mL). Nitrogen gas was bubbled through the solution within 10 min under sonication for removal of the dissolved oxygen prior to irradiation using a 125 W HPMV lamp (10 h monitored by TLC). After completion of the reaction, the excess of iodine was removed by washing the solution with aqueous $Na_2S_2O_3$ followed by distilled water. The organic layer was concentrated under the reduced pressure to obtain the crude product. The crude product purified by column chromatography over silica gel using petroleum ether/ethyl acetate (98:2) as eluent to obtained a pale yellow solid. For details of separation of the four compounds, see the Supporting Information. Overall yield = 0.077 g (44%, mixture of four compounds **7**−**10**).

Angular−angular Isomer (7). R_f = 0.22 (5:95 EtOAc/petroleum ether). Physical state = yellow solid. Mp = 260−262 °C. ^{1}H NMR (400 MHz, $CDCl_3$): δ 8.32 (d, J = 8.4 Hz, 2H), 8.21 (d, J = 8.4 Hz, 2H), 8.04 (d, J = 8.4 Hz, 2H), 7.58 (d, J = 8.4 Hz, 2H), 7.55 (d, J = 8.4 Hz, 2H), 7.42 (d, J = 8.4 Hz, 2H), 7.31 (d, J = 7.6 Hz, 2H), 6.77−6.73 (m, 2H), 6.11 (d, J = 8.4 Hz, 2H), 5.62−5.58 (m, 2H), 5.01−4.97 (m, 2H), 2.35−2.26 (m, 2H), 1.75−1.66 (m, 2H)1.14 (t, J = 7.6 Hz, 3H). $^{13}C\{^1H\}$ (100 MHz, $CDCl_3$): δ 137.6, 129.6, 129.2, 127.8, 127.4, 126.4, 126.2, 126.1 (2C), 125.9, 125.0, 124.6 (2C), 123.9, 123.8, 121.6, 118.7, 108.9, 43.7, 32.3, 20.8, 14.1. IR (KBr): 3042, 2956, 2928, 2868, 1619, 1577, 1527, 1490, 1463, 1439, 1360, 1335, 1287, 1251, 952, 910, 882, 777, 748, 628, 542 cm^{-1}. HRMS (APCI): m/z calcd for $C_{40}H_{29}N$ $[M + H]^+$ 524.2373, found 524.2372. HPLC conditions: two well-separated peaks [column: Chiralcel OD-H; IPA in hexane (10%), 1.0 mL/min, UV 254 nm, 7.33 and 11.71 min].

Angular−linear Isomer (8). R_f = 0.20 (5:95 EtOAc/petroleum ether). Physical state = yellow solid. Mp = 240 °C. ^{1}H NMR (400 MHz, $CDCl_3$): δ 9.47 (d, J = 8.4 Hz, 1H), 9.13 (s, 1H), 8.32 (d, J = 8.8 Hz, 1H), 8.19−8.03 (m, 6H), 7.92−7.69 (m, 5H), 7.69−7.65 (m, 1H), 7.58−7.56 (m, 1H), 7.52 (d, J = 8.4 Hz, 1H), 7.32 (d, J = 8.8 Hz, 1H), 7.14 (s, 1H), 7.13−7.09 (m, 1H), 4.62−4.58 (m, 2H), 2.14−2.09 (m, 2H), 1.68−1.58 (m, 2H), 0.11 (t, J = 7.2 Hz, 3H). $^{13}C\{^1H\}$ (100 MHz, $CDCl_3$): δ 142.6, 139.6, 133.3, 132.6, 131.8, 130.7 (2C), 130.0, 129.1, 128.9, 128.7, 128.3, 128.2, 128.0, 127.9, 127.7, 127.6, 127.2, 127.0, 126.9, 126.6, 126.3 (2C), 125.9, 125.7, 125.6, 125.4, 125.3, 125.1, 125.0, 123.6, 123.5, 123.2, 117.4, 110.1, 105.2, 43.2, 31.3, 20.8, 14.1. IR (KBr): 3045, 2956, 2928, 1619, 1577, 1527, 1463, 1441, 1360, 1337, 1287, 1251, 911, 882, 777, 748, 542 cm^{-1}. HRMS (APCI): m/z calcd for $C_{40}H_{29}N$ $[M + H]^+$ 524.2372, found 524.2372. HPLC conditions: two well-separated peaks [Column: Chiralcel OD-H; IPA in hexane (10%), 1.0 mL/min, UV 254 nm, 9.04 and 21.19 min].

Linear−linear Isomer (9). R_f = 0.20 (5:95 EtOAc/petroleum ether, appeared as a fluorescent green spot in long wavelength UV and appeared as a very faint spot in short wavelength UV). Physical state = yellow solid. Mp = 265 °C. ^{1}H NMR (400 MHz, $CDCl_3$): δ 9.41 (δ, J = 8.4 Hz, 2H), 9.13 (s, 2H), 8.91 (s, 2H), 8.17 (d, J = 8.4 Hz, 2H), 8.11 (dd, J = 8.0, 1.2 Hz, 2H), 7.97 (d, J = 8.8 Hz, 2H), 7.92 (d, J = 8.4

DOI: 10.1021/acs.joc.6b01395
J. Org. Chem. 2016, 81, 7751−7759

Hz, 2H), 7.79 (d, J = 8.8 Hz, 2H), 7.78−7.74 (m, 2H), 7.70−7.66 (m, 2H), 4.62 (t, J = 6.8 Hz, 2H), 2.19−2.12 (m, 2H),1.72−1.63 (m, 2H), 1.11 (t, J = 7.2 Hz, 3H). $^{13}C\{^1H\}$ (100 MHz, $CDCl_3$): δ 142.5, 133.4, 131.2, 130.7, 130.0, 128.7, 128.3, 127.7, 127.3, 127.2, 127.1, 126.9, 126.0, 125.5, 123.8, 123.5, 120.3, 105.1, 43.3, 30.9, 20.9, 14.1. IR (KBr): 3041, 2953, 2861, 2369, 1684, 1615, 1430, 1262, 1198, 1132, 881, 829, 790, 745, 623, 539 cm^{-1}. HRMS (ESI): m/z calcd for $C_{40}H_{29}N$ $[M + Na]^+$ 546.2190, found 546.2192

Angular−linear Fused Compound (10). R_f = 0.20 (5:95, EtOAc/petroleum ether). Physical state = yellow solid. Mp = 260 °C dec. ^1H NMR (400 MHz, $CDCl_3$): δ 9.32 (δ, J = 8.4 Hz, 1H), 8.87 (s, 1H), 8.12 (d, J = 8.8 Hz, 1H), 8.06 (dd, J = 8.0, 1.2 Hz, 1H), 7.89 (d, J = 8.4 Hz, 1H), 7.83−7.69 (m, 8H), 7.66−7.61 (m, 2H), 7.56 (d, J = 8.4 Hz, 1H), 7.49 (t, J = 7.6 Hz, 1H), 7.39 (d, J = 9.2 Hz, 1H), 4.48−4.34 (m, 2H), 2.07−1.93 (m, 2H), 1.55−1.54 (m, 2H merged with water peak), 1.05 (t, J = 7.2 Hz, 3H). $^{13}C\{^1H\}$ (100 MHz, $CDCl_3$): δ 144.3, 139.9, 138.6, 137.5 (2C), 136.1, 135.8, 133.3 (2C), 133.0, 132.9, 132.6, 131.6, 131.2, 130.6 (2C), 129.7, 128.7 (2C), 128.6, 128.4, 128.3, 128.0, 127.1 (2C), 126.8, 126.4 (2C), 126.0, 125.8, 125.3, 125.2, 121.9, 119.6, 109.8, 105.3, 43.0, 31.2, 20.6, 14.0. IR (KBr): 3043, 2973, 2861, 2365, 1684, 1615, 1431, 1262, 1198, 1132, 881, 829, 790, 745, 627, 539 cm^{-1}. HRMS (ESI): m/z calcd for $C_{40}H_{27}N$ $[M + H]^+$ 522.2223, found 522.2216.

■ ASSOCIATED CONTENT

Supporting Information

The Supporting Information is available free of charge on the ACS Publications website at DOI: 10.1021/acs.joc.6b01395.

X-ray data for compound **7** (CIF)
X-ray data for compound **8** (CIF)
Full experimental details, analytical data, spectral reproductions, and details of X-ray structure data (PDF)
X-ray data for compound **9** (CIF)
X-ray data for compound **10** (CIF)

■ AUTHOR INFORMATION

Corresponding Author

*Tel: +91-265-2795552. E-mail: avbedekar@yahoo.co.in.

Notes

The authors declare no competing financial interest.

■ ACKNOWLEDGMENTS

We are grateful to Science and Engineering Research Board (SERB), New Delhi, for supporting this work under a sponsored scheme (No. SR/S1/OC-74/2012) and DST-PURSE for the single-crystal X-ray diffraction facility installed in the Faculty of Science. We thank the Council of Scientific and Industrial Research (CSIR), New Delhi, for the award of a Junior Research Fellowship to G.M.U. We are also grateful to Dr. Amitava Das, CSMCRI, Bhavnagar, Dr. Firasat Hussain, University of Delhi and Dr. Hemant Mande for their timely help in measuring quantum yield and refining some of the crystal structure data.

■ REFERENCES

(1) (a) Grimme, S.; Harren, J.; Sobanski, A.; Vögtle, F. *Eur. J. Org. Chem.* **1998**, *1998*, 1491. (b) Urbano, A. *Angew. Chem., Int. Ed.* **2003**, *42*, 3986. (c) Collins, S. K.; Vachon, M. P. *Org. Biomol. Chem.* **2006**, *4*, 2518. (d) Rajca, A.; Miyasaki, M. In *Functional Organic Materials*; Muller, T. J. J., Bunz, U. H. F., Eds.; Wiley-VCH: Weinheim, 2007; p 547. (e) Dumitrascu, F.; Dumitrescu, D. G.; Aron, I. *Arkivoc* **2010**, 1. (f) Shen, Y.; Chen, C.-F. *Chem. Rev.* **2012**, *112*, 1463. (g) Gingras, M. *Chem. Soc. Rev.* **2013**, *42*, 968. (h) Gingras, M.; Félix, G.; Peresutti, R. *Chem. Soc. Rev.* **2013**, *42*, 1007. (i) Gingras, M. *Chem. Soc. Rev.* **2013**, *42*, 1051.

(2) (a) Oyama, H.; Nakano, K.; Harada, T.; Kuroda, R.; Naito, M.; Nobusawa, K.; Nozaki, K. *Org. Lett.* **2013**, *15*, 2104. (b) Hua, W.; Liu, Z.; Duan, L.; Dong, G.; Qiu, Y.; Zhang, B.; Cui, D.; Tao, X.; Cheng, N.; Liu, Y. *RSC Adv.* **2015**, *5*, 75.

(3) (a) Field, J. E.; Muller, G.; Riehl, J. P.; Venkataraman, D. *J. Am. Chem. Soc.* **2003**, *125*, 11808−11809. (b) Sawada, Y.; Furumi, S.; Takai, A.; Takeuchi, A.; Takeuchi, M.; Noguchi, K.; Tanaka, K. *J. Am. Chem. Soc.* **2012**, *134*, 4080. (c) Shyam Sundar, M.; Talele, H. R.; Mande, H. M.; Bedekar, A. V.; Tovar, R. C.; Muller, G. *Tetrahedron Lett.* **2014**, *55*, 1760. (d) Nakamura, K.; Furumi, S.; Takeuchi, M.; Shibuya, T.; Tanaka, K. *J. Am. Chem. Soc.* **2014**, *136*, 5555. (e) Morisaki, Y.; Gon, M.; Sasamori, T.; Tokitoh, N.; Chujo, Y. *J. Am. Chem. Soc.* **2014**, *136*, 3350.

(4) (a) Morrison, D. J.; Trefz, T. K.; Piers, W. E.; McDonald, R.; Parvez, M. *J. Org. Chem.* **2005**, *70*, 5309. (b) Wang, Z. Y.; Todd, E. K.; Meng, X. S.; Gao, J. P. *J. Am. Chem. Soc.* **2005**, *127*, 11552. (c) Rajapakse, A.; Gates, K. S. *J. Org. Chem.* **2012**, *77*, 3531. (d) Li, M.; Niu, Y.; Zhu, X.; Peng, Q.; Lu, H.-Y.; Xia, A.; Chen, C.-F. *Chem. Commun.* **2014**, *50*, 2993. (e) Li, M.; Yao, W.; Chen, J.-D.; Lu, H.-Y.; Zhao, Y.; Chen, C.-F. *J. Mater. Chem. C* **2014**, *2*, 8373. (f) Yamamoto, Y.; Sakai, H.; Yuasa, J.; Araki, Y.; Wada, T.; Sakanoue, T.; Takenobu, T.; Kawai, T.; Hasobe, T. *Chem. - Eur. J.* **2016**, *22*, 4263.

(5) (a) Nuckolls, C.; Katz, T. J.; Castellanos, L. *J. Am. Chem. Soc.* **1996**, *118*, 3767. (b) Nuckolls, C.; Katz, T. J. *J. Am. Chem. Soc.* **1998**, *120*, 9541. (c) Verbiest, S.; Van Elshocht, M.; Kauranen, L.; Hellemans, J.; Snauwaert, C.; Nuckolls, C.; Katz, T. J.; Persoons, A. *Science* **1998**, *282*, 913. (d) Hassey, R.; Swain, E. J.; Hammer, N. I.; Venkataraman, D.; Barnes, M. D. *Science* **2006**, *314*, 1437. (e) Hassey, R.; McCarthy, K. D.; Basak, D.; Venkataraman, D.; Barnes, M. D.; Swain, E. *Chirality* **2008**, *20*, 1039. (f) Kaseyama, T.; Furumi, S.; Zhang, X.; Tanaka, K.; Takeuchi, M. *Angew. Chem., Int. Ed.* **2011**, *50*, 3684. (g) Roose, J.; Achermann, S.; Dumele, O.; Diederich, F. *Eur. J. Org. Chem.* **2013**, *2013*, 3223. (h) Richardson, R. D.; Baud, M. G. J.; Weston, C. E.; Rzepa, H. S.; Kuimova, M. K.; Fuchter, M. J. *Chem. Sci.* **2015**, *6*, 3853.

(6) Bosson, J.; Gouin, J.; Lacour, J. *Chem. Soc. Rev.* **2014**, *43*, 2824.

(7) Caronna, T.; Sinisi, R.; Catellani, M.; Malpezzi, L.; Meille, S. V.; Mele, A. *Chem. Commun.* **2000**, 1139.

(8) Bunz, U. H. F. *Angew. Chem., Int. Ed.* **2010**, *49*, 5037.

(9) (a) Tsuji, H.; Mitsui, C.; Ilies, L.; Sato, Y.; Nakamura, E. *J. Am. Chem. Soc.* **2007**, *129*, 11902. (b) Mitsui, C.; Soeda, J.; Miwa, K.; Tsuji, H.; Takeya, J.; Nakamura, E. *J. Am. Chem. Soc.* **2012**, *134*, 5448. (c) Nakano, M.; Niimi, K.; Miyazaki, E.; Osaka, I.; Takimiya, K. *J. Org. Chem.* **2012**, *77*, 8099.

(10) Shyam Sundar, M.; Bedekar, A. V. *Org. Lett.* **2015**, *17*, 5808.

(11) Nakano, K.; Oyama, H.; Nishimura, Y.; Nakasako, S.; Nozaki, K. *Angew. Chem.* **2012**, *124*, 719.

(12) (a) Nakano, K.; Hidehira, Y.; Takahashi, K.; Hiyama, T.; Nozaki, K. *Angew. Chem., Int. Ed.* **2005**, *44*, 7136. (b) Shiraishi, K.; Rajca, A.; Pink, M.; Rajca, S. *J. Am. Chem. Soc.* **2005**, *127*, 9312. (c) Nakano, K.; Oyama, H.; Nishimura, Y.; Nakasako, S.; Nozaki, K. *Angew. Chem., Int. Ed.* **2012**, *51*, 695. (d) Upadhyay, G. M.; Talele, H. R.; Sahoo, S.; Bedekar, A. V. *Tetrahedron Lett.* **2014**, *55*, 5394. (e) Chercheja, S.; Klívar, J.; Janccřík, A.; Rybáček, J.; Salzl, S.; Tarábek, J.; Pospíšil, L.; Chocholoušová, J. V.; Vasek, J.; Pohl, R.; Císařová, I.; Starý, I.; Stará, G. I. *Chem. - Eur. J.* **2014**, *20*, 8477. (f) Ben Braiek, M.; Aloui, F.; Ben Hassine, B. *Tetrahedron Lett.* **2016**, *57*, 2763.

(13) Kötzner, L.; Webber, M. J.; Martínez, A.; De Fusco, C.; List, B. *Angew. Chem., Int. Ed.* **2014**, *53*, 5205.

(14) Hoffmann, N. *J. Photochem. Photobiol., C* **2014**, *19*, 1.

(15) Laarhoven, W. H.; Cuppen, J. H. M.; Nivard, R. J. F. *Tetrahedron* **1970**, *26*, 4865.

(16) (a) Mallory, F. B.; Mallory, C. W. *Organic Reactions*; Wiley: New York, 1984; Vol. *30*, p 48. (b) Mallory, F. B.; Mallory, C. W. *Organic Reactions*; Wiley: New York, 1984; Vol. *30*, p 49.

(17) Roose, J.; Achermann, S.; Dumele, O.; Diederich, F. *Eur. J. Org. Chem.* **2013**, *2013*, 3223.

DOI: 10.1021/acs.joc.6b01395
J. Org. Chem. 2016, 81, 7751−7759

(18) Dreher, S. D.; Weix, D. J.; Katz, T. J. *J. Org. Chem.* **1999**, *64*, 3671.
(19) Zhao, T.; Liu, Z.; Song, Y.; Xu, W.; Zhang, D.; Zhu, D. *J. Org. Chem.* **2006**, *71*, 7422.
(20) Talele, H. R.; Gohil, M. J.; Bedekar, A. V. *Bull. Chem. Soc. Jpn.* **2009**, *82*, 1182.
(21) Cabri, W.; Candiani, I.; Bedeschi, A.; Penco, S.; Santi, R. *J. Org. Chem.* **1992**, *57*, 1481.
(22) (a) Dietz, F.; Scholz, M. *Tetrahedron* **1968**, *24*, 6845. (b) Laarhoven, W. H.; Cuppen, T. J. H. M.; Nivard, R. J. F. *Tetrahedron* **1970**, *26*, 1069. (c) Xue, X.; Scott, L. T. *Org. Lett.* **2007**, *9*, 3937 and references cited therein.
(23) Bas, G. L.; Navaza, A.; Knossow, D. R. C. M. *Cryst. Struct. Commun.* **1976**, *5*, 713.
(24) (a) Martin, R. H.; Eyndels, C.; Defay, N. *Tetrahedron* **1974**, *30*, 3339. (b) Laarhoven, W. H.; Cuppen, T. J. H. M.; Nivard, R. J. F. *Tetrahedron* **1974**, *30*, 3343. (c) Marsh, W.; Dunitz, J. D. *Bull. Soc. Chim. Belg.* **1979**, *88*, 847.
(25) Crystallographic data for the structures of compounds **7**−**10** have been deposited with the Cambridge Crystallographic Data Centre. Copies can be obtained from http://www.ccdc.cam.ac.uk/conts/retrieving.html or from the Cambridge Crystallographic Data Centre, 12 Union Road, Cambridge CD21EZ, UK (fax: + 44-1223-336-033; e-mail: deposit@ccdc.cam.ac.uk).
(26) Wismonski-Knittel, T.; Fischer, G.; Fischer, E. J. *J. Chem. Soc., Perkin Trans. 2* **1974**, 1930.
(27) Pozo, I.; Cobas, A.; Peña, D.; Guitián, E.; Pérez, D. *Chem. Commun.* **2016**, *52*, 5534.
(28) For experimental details and spectral reproductions, see the Supporting Information.
(29) Upadhyay, G. M.; Bedekar, A. V. *Tetrahedron* **2015**, *71*, 5644.
(30) (a) Li, Y.; Ding, J.; Day, M.; Tao, Y.; Lu, J.; D'iorio, M. *Chem. Mater.* **2004**, *16*, 2165. (b) Vander Donckt, E. V.; Nasielski, J.; Greenleaf, J. R.; Birks, J. B. *Chem. Phys. Lett.* **1968**, *2*, 409. (c) Yamamoto, Y.; Sakai, H.; Yuasa, J.; Araki, Y.; Wada, T.; Sakanoue, T.; Takenobu, T.; Kawai, T.; Hasobe, T. *Chem. - Eur. J.* **2016**, *22*, 4263. (d) Oyler, K. D.; Coughlin, F. J.; Bernhard, S. *J. Am. Chem. Soc.* **2007**, *129*, 210.
(31) (a) Chuang, C. N.; Wang, Y. X.; Chen, S. H.; Huang, J. J.; Leung, M. K.; Hsieh, K. H. *Polymer* **2012**, *53*, 4983. (b) Sket, B.; Zupan, M. *J. Org. Chem.* **1986**, *51*, 929. (c) Guan, B.; Xing, D.; Cai, G.; Wan, X.; Yu, N.; Fang, Z.; Yang, L.; Shi, Z. *J. Am. Chem. Soc.* **2005**, *127*, 18004. (d) Klahn, P.; Erhardt, H.; Kotthaus, A.; Kirsch, S. F. *Angew. Chem., Int. Ed.* **2014**, *53*, 7913.

DOI: 10.1021/acs.joc.6b01395
J. Org. Chem. 2016, 81, 7751−7759